WILEY | Hindawi

Research Article

A Wideband Highly Efficient Omnidirectional Compact Antenna for WiMAX/Lower 5G Communications

Liton Chandra Paul [iD],[1] **Sarker Saleh Ahmed Ankan** [iD],[1] **Tithi Rani** [iD],[2]
Muharrem Karaaslan [iD],[3] **Md. Najmul Hossain** [iD],[1] **Ahmed Jamal Abdullah Al-Gburi** [iD],[4]
Himel Kumar Saha [iD],[1] **and Fatih Özkan Alkurt**[3]

[1]*Electrical, Electronic and Communication Engineering, Pabna University of Science Technology, Pabna 6600, Bangladesh*
[2]*Electronics and Telecommunication Engineering, Rajshahi University of Engineering and Technology, Rajshahi 6204, Bangladesh*
[3]*Electrical and Electronics Engineering, Iskenderun Technical University, Hatay 31200, Turkey*
[4]*Center for Telecommunication Research & Innovation (CeTRI), Faculty of Electrical and Electronic Engineering
Technology (FTKEE), Melaka 76100, Malaysia*

Correspondence should be addressed to Liton Chandra Paul; litonpaulete@gmail.com

Microstrip patch antenna (MPA) is widely used for different wireless communications such as WiMAX and fifth generation (5G). In this paper, a wideband, highly efficient, omnidirectional, compact novel patch antenna has been designed and reported for WiMAX/lower 5G communications. The proposed compact MPA is made on Rogers RT 5880 (ε_r = 2.2 and tan (δ) = 0.0009). The physical volume of the MPA is compact ($32 \times 32 \times 0.79$ mm^3). The MPA consists of seven small square-shaped elements that are diagonally connected with each other. The 7-element antenna works at 3.592 GHz with a suitable reflection coefficient of -46.78 dB and a -10 dB bandwidth (BW) of 1.40 GHz, covering 3.10-4.50 GHz. The apex gain (G) and the directivity (D) of the designed prototype are 3.90 dB and 4.20 dBi, respectively. The antenna maintains a high efficiency of 94-98% over the 3.10-4.50 GHz operating range. The VSWR of the antenna is close to unity, which is 1.0092 at 3.592 GHz. Initially, CST is used to design the antenna, and then, all the properties have been buttressed by using high frequency structure simulator (HFSS). Finally, a prototype of the compact 7-element antenna has been developed and measured. Owing to getting good results for the intended applications, the presented compact antenna can be a reliable candidate for WiMAX (3.4-3.6 GHz) and lower 5G (3.3-4.2 GHz).

1. Introduction

There are billions of people in the world, and they are very far from each other. In the early ages, it was difficult to connect with each other through wired communication. This difficulty is solved by wireless communication. Now we can connect to any network without any hassle. No presetup connection is needed here. Therefore, in the telecommunication sector, wireless communication is the fastest growing and most promising technology [1]. Strong wireless communication networks, including Internet of Things (IoT), artificial intelligence, and 5G, are essential to the development of powerful new technologies [2, 3]. 5G is mainly the fifth generation of technology in cellular network systems. It comes after four generations of networking. These networks were 1G, 2G, 3G, and 4G. Here, every generation is faster than the previous one [4]. Because the aim of today's technology is the fastest data transfer, these things make 5G different from other generations because of its capacity and latency [5, 6]. The maximum capacity in fifth generation ultrawideband (UWB) is in gigabits per second (Gbps), which was megabits per second (mbps) in the previous generation (4G) [7]. They enable the instantaneous connection of billions of devices for the purpose of gathering and sharing

information. For transferring these huge amounts of data, the fifth generation uses various frequency spectrums. These spectrums vary from country to country. In many countries, 5G systems are still in trial, and frequency bands have yet to be finalized. Among them, the most common lower 5G band is N77 [8]. It ranges from 3.3 to 4.2 GHz. It also falls within the C-band. The N78 band is also included here, which ranges from 3.3 to 3.8 GHz. These bands are less complex in the development of infrastructure, deployment, and future network enhancements in comparison to the upper band [9]. Because they are less than 6 GHz, these bands are also familiar as "sub-6 GHz" bands. Around this range, we can get another band of 3.4–3.6 GHz, which is one of the three spectrums of WiMAX. Based on the IEEE 802.16, the WiMAX progeny of wireless broadband technologies offers solutions for the physical layer and media access control. It offers fast web surfing without being connected through cable or a digital subscriber line (DSL) [10, 11]. The infrastructure of WiMAX is very easy and flexible [12, 13]. It can handle multiple users exchanging data at the same time [14]. Users could afford this dependable, secure technology [15, 16]. Orthogonal frequency division multiplexing (OFDM) is integrated with WiMAX technology to enable it to provide high speed data [17]. To design and simulate this technology, various user-friendly software packages are now available on the market. In [18], the authors used CST microwave studio and advanced design system (ADS) electromagnetic solver for designing the antenna. The simulated result slightly varies from software to software. But it does not change the whole output of a well-designed antenna. An antenna with dimensions of $30 \times 45 \times 1.6$ mm^3 works at two resonant points. These are 2.45 GHz and 5.8 GHz. The return losses at these points are around -30 dB and -23 dB, respectively. The design covers a good bandwidth of 0.48 GHz and 1.89 GHz, but the gain of the antenna is medium. A high gain antenna is discussed in [19]. The gain of the MPA is 6.8 dB with a huge substrate dimension of $100 \times 100 \times 1.6$ mm^3. It increases the cost of fabrication. It is also a dual-band antenna whose resonance points are 2.45 GHz and 3.50 GHz. This antenna provides 70% efficiency with a good reflection coefficient of -40 dB and -25 dB. The authors in [20] proposed a small MPA for 5G applications. They used Ansoft's HFSS to model the antenna. This compact size antenna ($50 \times 50 \times 1.6$ mm^3) provides a slightly small BW of 0.25 GHz with a considerable gain of 3 dB. The gain of work in [21] is comparatively low (2.3 dB), but the size of the MPA is compact. The dimensions of the MPA are $22.5 \times 10.7 \times 1.6$ mm^3 with a low efficiency of 73%. The compact size of the MPA will reduce the fabrication cost. It resonates at 3.8 GHz with a good bandwidth of 0.8 GHz. The reflection coefficient at the resonant point is around -25 dB, which is good for applications. The antenna presented in [22] resonates at 3.4 GHz. It is a narrowband, compact-size antenna with a good gain. The height of the substrate is slightly thicker (3.2 mm). The gain of 4.8 dB makes it a good candidate for 5G applications.

This work is designed and investigated by CST-MWS and HFSS. The volume of the Rogers RT 5880 substrate is $32 \times 32 \times 0.79$ mm^3. This 7-element MPA covers the band of 3.10-4.50 GHz. It exhibits a reflection coefficient of -46.78 dB at 3.592 GHz. This antenna provides a good maximum efficiency of 98% with a stable peak gain and directivity of 3.90 dB and 4.2 dBi, respectively. A structural preview of the proposed 7-element MPA is given in Section 2. Section 3 deals with the parametric study and an analytical discussion of the obtained results. The last section of this paper (Section 4) terminates with conclusive expressions.

2. Structure and Evolution Steps of the Compact Antenna

This section shows the proposed compact antenna's evolution steps and different views from different angles with geometrical measurement. It gives us a total idea of the geometrical structure of the antenna. Initially, a small square-shaped MPA is designed as presented in Figure 1(a). Equations (1) through (4) have been used to predict the antenna's initial dimensions. In step 2 of the design, two square-shaped elements of the same size are connected through corner edges to tune and improve performance, as shown in Figure 1(b). In steps 3 and 4, 5-element and 7-element diagonally connected antennas have been designed and optimized to tune in the lower 5G communication, as depicted in Figures 1(c) and 1(d), respectively. The antenna presented in step 4 is the final proposed antenna. Figures 2(a)–2(d) show the 3D view, amplified view of the patch element, back view, and fabricated prototype of the designed antenna, respectively. We have used CST-MWS to create and simulate the antenna model. The dimension of the substrate is $32 \times 32 \times 0.79$ mm^3. From the top view, we can also see the measurements of the feedline's length and width. The value of the feedline's width is taken to be 2.50 mm, which is related to the impedance matching of the MPA with a 50 Ω port impedance. The impedance of the investigated antenna should match the 50 Ω SMA connector. The length of the feedline is 14 mm. We have used copper (annealed) material for both radiating patch elements and a partial ground plane with a thickness of 0.035 mm. In the amplified view, half of the radiating patch elements are shown. The measurement is the same for the other half. Here, square-shaped radiating elements are diagonally connected to each other. The area of these single patch elements is 4×4 mm^2. It is simple and compact in structure. The ground layer's length is 17.10 mm, which is denoted by L_g.

$$\text{Patch width, } W_P = \frac{c}{2f_r}\sqrt{\frac{2}{\varepsilon_r + 1}}, \tag{1}$$

where c is the velocity of light, f_r is the resonance frequency, and ε_r is the dielectric constant [23].

$$\text{Length, } L = 0.412h\frac{(\varepsilon_{\text{reff}} + 0.3)\left((W_p/h) + 0.264\right)}{(\varepsilon_{\text{reff}} - 0.258)\left((W_p/h) + 0.8\right)}, \tag{2}$$

$$\text{Effective length, } L_{\text{eff}} = \frac{c}{2f_r\sqrt{\varepsilon_{\text{reff}}}}, \tag{3}$$

(a) 1-element (step 1)   (b) 3-element (step 2)   (c) 5-element (step 3)   (d) 7-element (step 4)

FIGURE 1: Evolution steps.

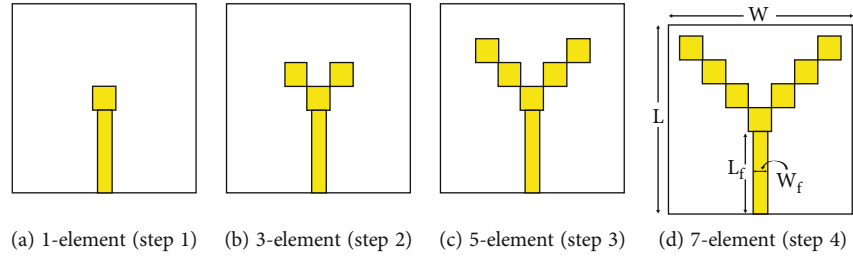

(a) 3D view   (b) Amplified view   (c) Back side
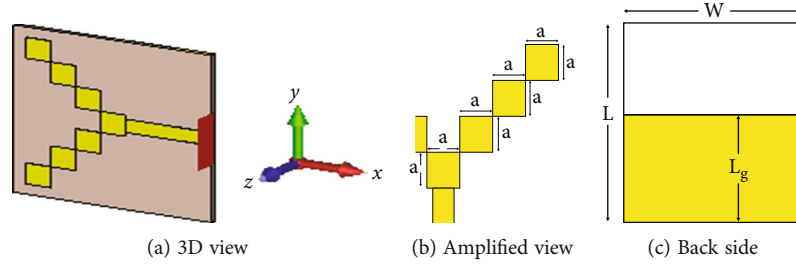

(d) 7-element prototype

FIGURE 2: Proposed 7-element antenna.

$$\text{Patch length, } L_p = L_{\text{eff}} - 2\Delta L. \quad (4)$$

3. Measurement, Parametric Study, and Discussion

A measurement setup of reflection loss occurring in the intended operating band is shown in Figure 3. The reflection loss can also be presented in terms of various names, such as $|S_{11}|$ parameters, return loss profile, or reflection coefficient. It can not be anyone's desire to cause more reflection at the operating band. Therefore, it is preferred to have a very low value of $|S_{11}|$ in the operating band. The amount of reflection coefficient in our proposed work is -46.78 dB as presented in Figure 4. The validation of the $|S_{11}|$ curve is performed by incorporating simulated results from the CST and HFSS softwares as well as measured result from the VNA (N5224A PNA microwave network analyzer, 43.5 GHz). There is very good agreement among them. The antenna resonates at 3.592 GHz, which is known as its resonance frequency. The -10 dB impedance BW is 1.40 GHz, where the lower and higher cut-off frequencies of the operating band are 3.10 GHz and 4.50 GHz, respectively. As we discussed in the earlier section, the compact antenna has
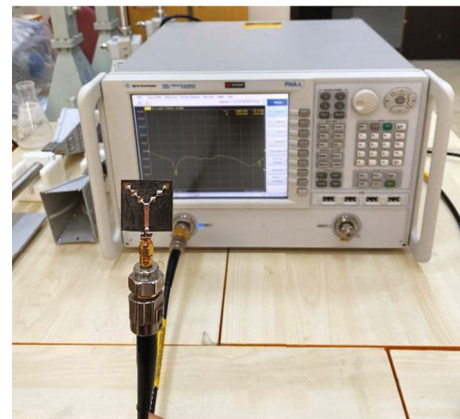

FIGURE 3: Reflection coefficient measurement using VNA.

been designed and presented in four steps. The impact of the number of square-shaped radiating elements on $|S_{11}|$ has been presented in Figure 5. At step 1, i.e., having a single element, the antenna shows very high reflection, which is not suitable to operate in the desired band. As the number
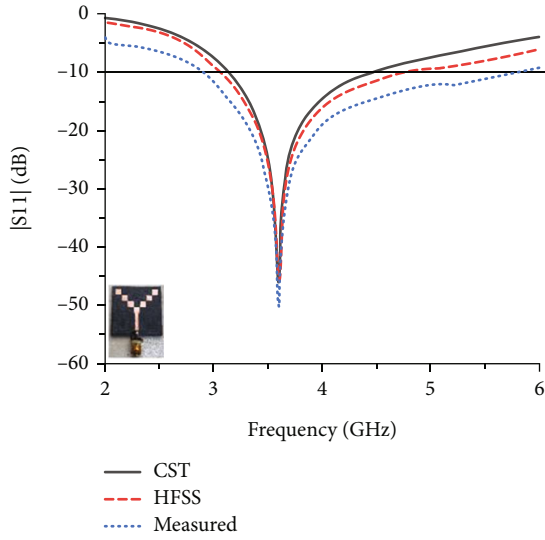
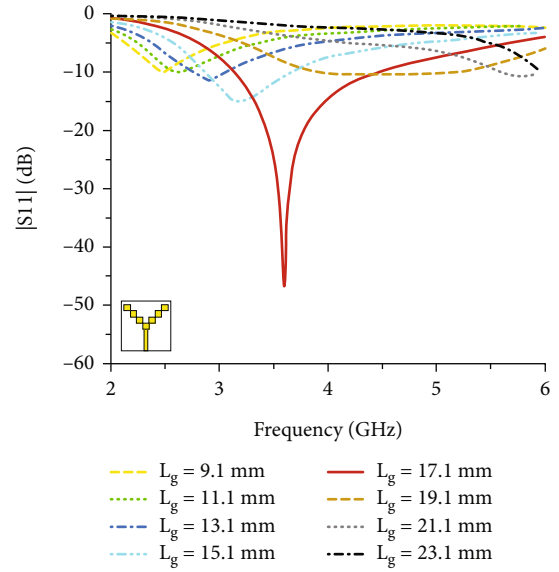Figure 4: $|S_{11}|$ curve validation.

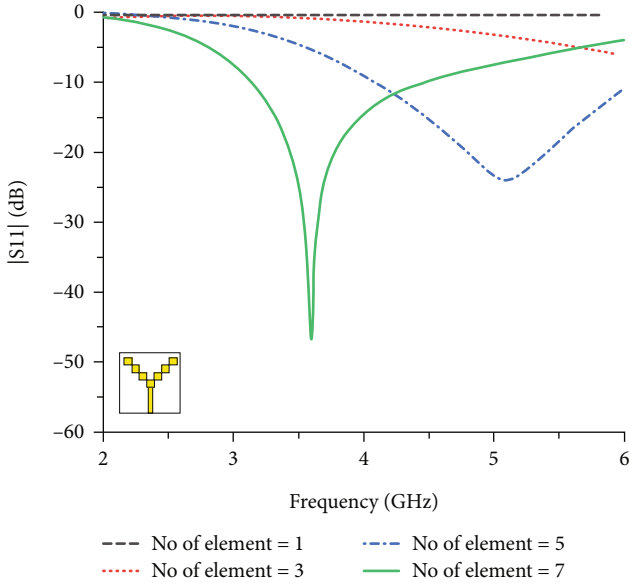Figure 6: $|S_{11}|$ curve and length of partial ground plane (L_g).

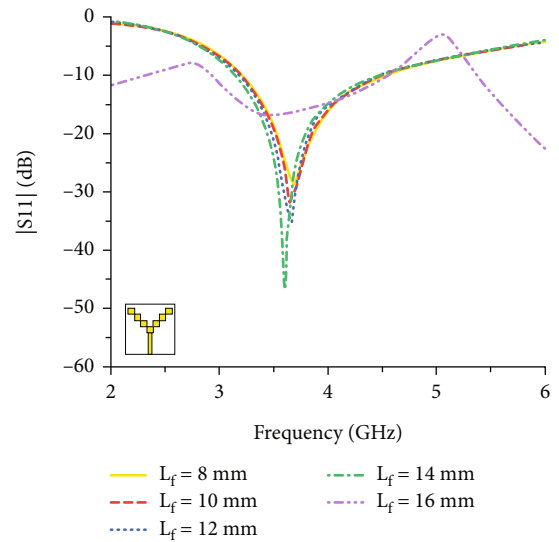Figure 5: $|S_{11}|$ curve and number of elements.

Figure 7: $|S_{11}|$ curve and length of feeder (L_f).

of square-shaped elements increases, the return loss decreases and tunes to the desired lower 5G operating band. During optimization of geometrical parameters, in order to achieve the lowest return loss, the partial ground plane's length (L_g) is optimized at 17.1 mm. Figure 6 presents $|S_{11}|$ from $L_g = 9.1$ mm to 23.1 mm with an augmentation of 2 mm. Both the length and width of the antenna's feeder have a vital influence on the impedance of the antenna. The optimized feeder length (L_f) is 14 mm, for which the 7-element MPA exhibits a maximum bandwidth of 1.40 GHz with a suitable reflection coefficient of -46.78 dB. The 7-element MPA shows lower bandwidth and higher return loss for all other values except $L_f = 14$ mm as presented in Figure 7.

Figure 8 expresses all the information about the gain and directivity of the MPA. 3D and Cartesian plots of gain and 3D directivity at 3.592 GHz are drawn in Figures 8(a)–8(c), respectively. The compact 7-element MPA exhibits omnidirectional characteristics with a gain of 2.766 dB and directivity of 2.929 dB at 3.592 GHz. At 3.592 GHz and $\varphi = 90°$, the Cartesian gain of the squared-shaped 7-element MPA with respect to the theta (θ) in the range 0°-180° is presented. The primary lobe size and direction of the gain are 2.72 dB and 180°, respectively. The gain of the 7-element MPA is also estimated by HFSS and measured in the antenna laboratory in the range of 2–6 GHz. The minimum gain is 2.70 dB at the lower cut-off frequency of 3.10 GHz, and the maximum gain is 3.90 dB at the higher cut-off frequency of 4.50 GHz. As shown in Figure 8(d), the measured gain parallels the predicted gains using both CST and HFSS. The

Farfield (f = 3.592) [1]
Type   Farfield
Approximation   Enabled (kR >> 1)
Component   Abs
Output   Gain
Frequency   3.592 GHz
Rad. effic.   −0.1628 dB
Tot. effic.   −0.1628 dB
Gain   2.766 dB

(a) Gain (3D) at 3.592 GHz

Frequency = 3.592 GHz
Main lobe magnitude = 2.72 dB
Main lobe direction = 180.0 deg.

(b) Cartesian gain at 3.592 GHz

Farfield (f = 3.592) [1]
Type   Farfield
Approximation   Enabled (kR >> 1)
Component   Abs
Output   Directivity
Frequency   3.592 GHz
Rad. effic.   −0.1628 dB
Tot. effic.   −0.1628 dB
Dir.   2.929 dB

(c) Directivity (3D) at 3.592 GHz

CST
HFSS
Measured

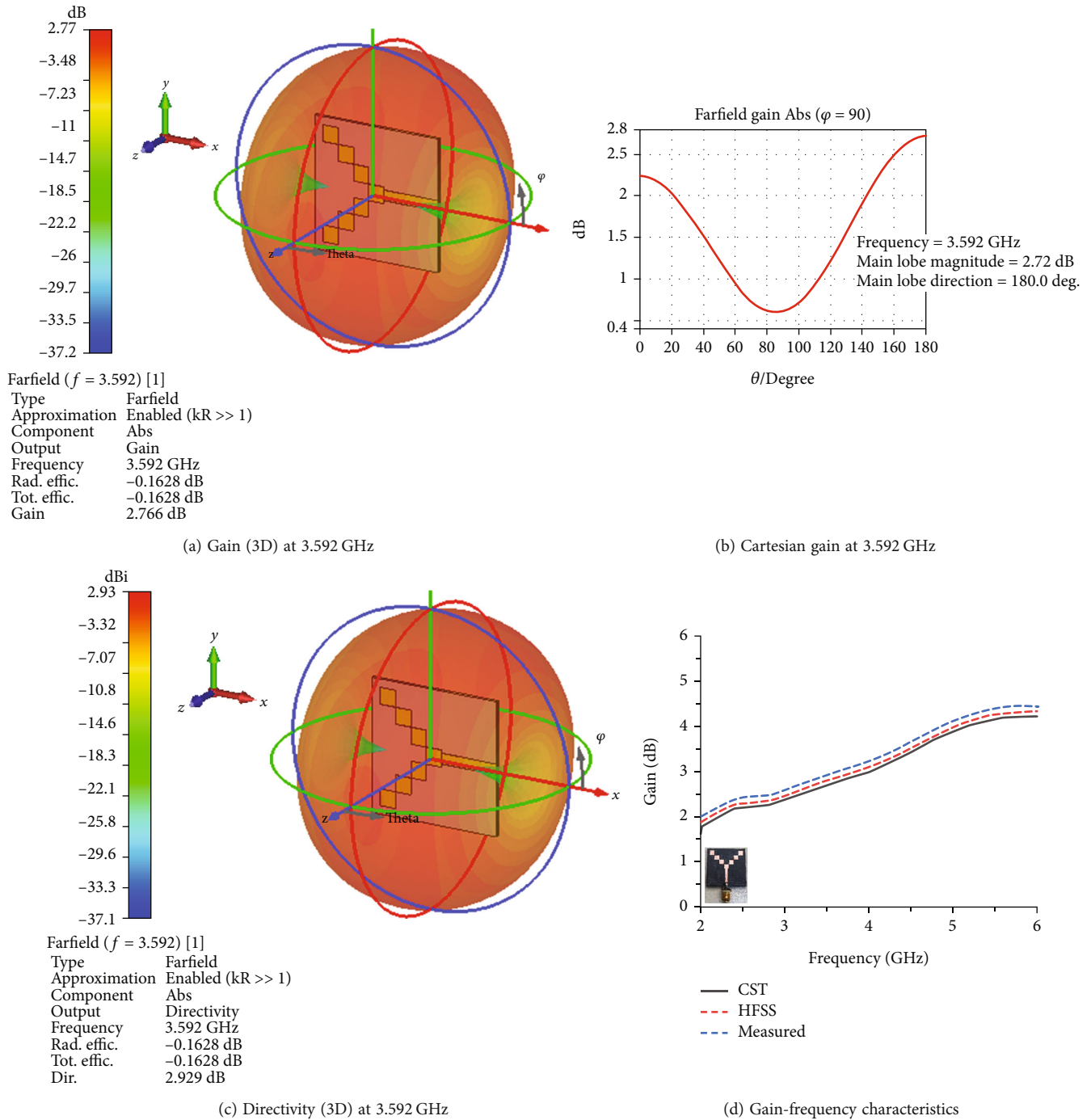(d) Gain-frequency characteristics

Figure 8: Gain and directivity profile of the compact antenna.

obtained gain is very standard for using the antenna in applications where omnidirectional properties are needed. There is a linear relationship between the gain and the number of elements in the compact antenna. The antenna possesses a comparatively higher gain for the antenna with seven elements than others, as depicted in Figure 9. The elements of the MPA are not increased further to keep the antenna size compact and ensure omnidirectional radiation properties for the use of WiMAX and lower 5G communications. The study of the impact of the L_g and L_f on the gain of

the compact antenna has also been performed. For L_g = 23.1 mm, the gain at the lower cut-off frequency is comparatively low, whereas the gain at the higher cut-off frequency is comparatively high. Therefore, there is a huge difference between gains at lower and higher cut-off frequencies. With decreasing L_g, the gain is becoming more stable within the operating frequency range. Finally, the proposed compact antenna exhibits standard gain while maintaining an omnidirectional property for L_g = 17.1 mm, as drawn in Figure 10. The length of the
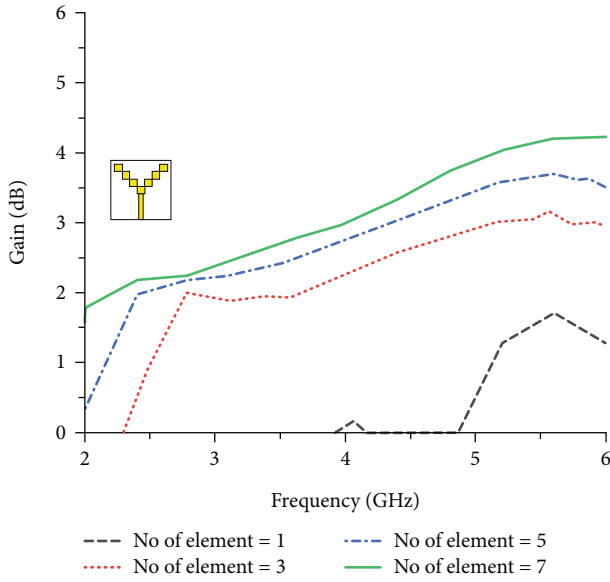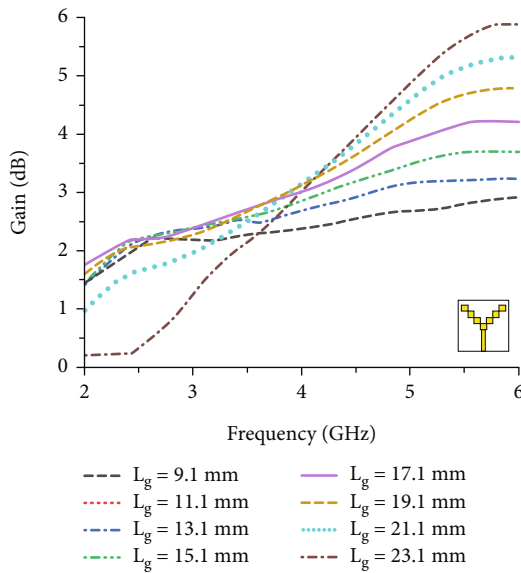
FIGURE 9: Gain and number of elements.

FIGURE 10: Gain and length of partial ground plane (L_g).
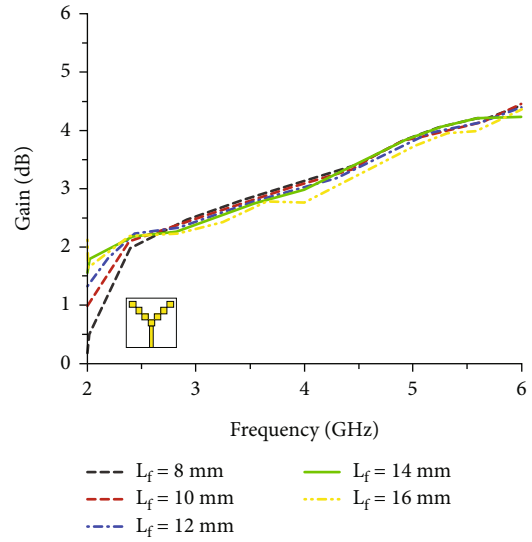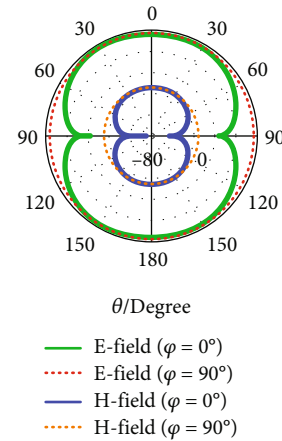

FIGURE 11: Gain and length of feeder (L_f).

FIGURE 12: E-field and H-field curves of the proposed antenna.
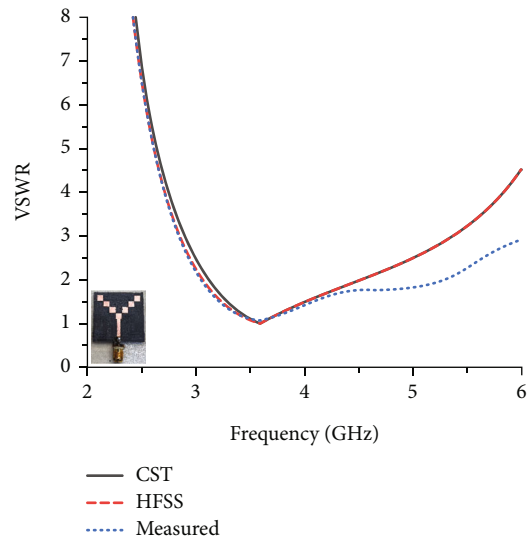
FIGURE 13: VSWR of the investigated MPA.

feeder (L_f) does not have a considerable impact on the gain of the designed compact antenna, as shown in Figure 11.

The electric and magnetic field patterns are enough to present the whole radiation pattern of the designed compact antenna. The E-field and H-field patterns of the antenna, which are taken at both $\phi = 0°$ and $\phi = 90°$, are drawn in Figure 12 for a resonant frequency of 3.592 GHz. The electric field's primary lobe sizes are the same as 17.5 dBV/m for both 0° and 90°. The angular width (3 dB) of the prime lobe direction at $\phi = 0°$ is 82.6°. The E-field pattern, which is 180°, achieves an excellent main lobe direction at $\phi = 90°$. Likewise, for H-field, the primary lobe size is -34 dBA/m for both $\phi = 0°$ and $\phi = 90°$. The main lobe direction of the magnetic field is a carbon copy of the electric field direction. The
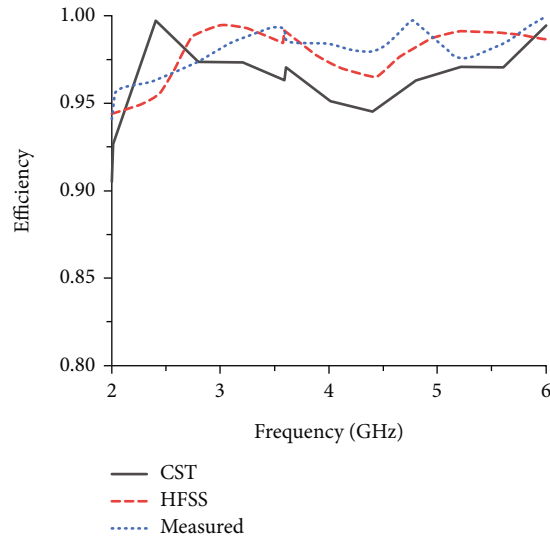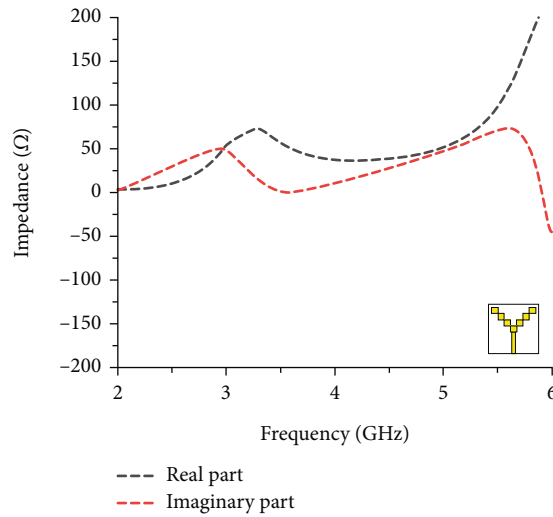
FIGURE 14: Efficiency of the MPA.

FIGURE 15: Z-parameters.

angular width (HPBW, 3 dB) at $\phi = 0°$ is 82.6°. The characteristics of E-field and H-field vividly express that the proposed compact 7-element MPA is an omnidirectional antenna. It emits power all around the x-axis.

Voltage standing wave ratio is referred to as VSWR. As drawn in Figure 13, the simulated and measured VSWR values of the recommended compact MPA are varied between 1 and 2 over the large 1.40 GHz operational bandwidth (3.10–4.50 GHz). The value of VSWR is 1.0092 at 3.592 GHz. Both the simulated and measured efficiencies of the compact antenna are high, as presented in Figure 14. The efficiency varies from 94% to 98% over the large 1.40 GHz bandwidth ranging from 3.10 to 4.50 GHz. We have a peak radiation efficiency of 98% at its resonant frequency of 3.592 GHz. The Z-parameters, including both real and imaginary parts at 3.592 GHz, are displayed in Figure 15. An antenna's impedance serves as an indicator of its resistance to electrical signals. The environment in

which an antenna is located, as well as its design and construction, has an effect on the antenna's capacity to transmit a signal. The power that an antenna absorbs and disperses when it comes into contact with an electromagnetic wave is both represented by the antenna impedance. The impedance values of the same antenna will vary depending on the electromagnetic radiation's varied wavelengths. The imaginary portion of the impedance corresponds to power held in the antenna's near field. Due to using a 50 Ω SMA connector for the input port, at 3.592 GHz, the real part would be approximately 50 Ω, and the imaginary value would be about 0 Ω. The real and imaginary parts of the compact MPA at 3.592 GHz are 49.978 Ω and 0.4333 Ω, respectively. Those are very close to the standard values.

Table 1 presents a comparison scenario with the state of the art of the related research works. Our proposed antenna possesses more compactness than all the cited works in the table except reference [22]. Though our design is almost

TABLE 1: Comparison with state of the art.

Parameter	[18]	[19]	[20]	[21]	[22]	Reference works [23]	[24]	[25]	[26]	[27]	[28]	Proposed work
No. of band	2	2	1	1	1	2	1	1	1	3	1	1
Resonant frequency (GHz)	2.45, 5.8	2.45, 3.50	≈3.44	3.8	3.4	2.475, 3.45	3.9	3.41, 3.83	2.1, 3.5	~1.3, ~2.4, ~3.8	3.47	3.592
Reflection coefficient (dB)	≈ -30, ≈ -23	-40, -25	≈ -24.5	≈ -25	< -10	~ -22	~ -38	-31.15	~ -38, ~ -22	~ -18, ~ -18, ~ -35	-23	-46.78
Bandwidth (GHz)	0.48, 1.89	0.3, 0.23	0.25	0.8	≈0.27	0.1, 0.36	1.08	0.72	1.95	0.23, 0.3, 0.7	1.01	1.40
Maximum gain (dB)	—	6.8	3	2.3	4.8	~4	6	2.5	4.044	5	4.08	3.90
Maximum efficiency (%)	—	70	—	73	—	—	—	—	92	80	—	98
Substrate	FR4	FR4	FR4	FR4	FR4	Rogers RT/ Duroid	ECCOSTOCK HIK	FR4	FR4	FR4	FR4	Rogers RT 5880
Substrate size ($L \times W \times h$) (mm^3)	30 × 45 × 1.6	100 × 100 × 1.6	50 × 50 × 1.6	22.5 × 10.7 × 1.6	34 × 34 × 3.2	46 × 46 × 3.175	35 × 35 × *	40 × 30 × 1.6	48 × 35 × 1.62	150 × 80 × 0.8	36 × 36 × 4	32 × 32 × 0.79
Year	2018	2019	2019	2020	2018	2021	2022	2020	2021	2019	2021	2023

N.B.: * means not available.

double in size than [22], the bandwidth of the proposed design, covering a range of 3.10–4.50 GHz, is almost double, with a maximum efficiency of 98% and a better reflection coefficient of -46.78 dB. It also shows a good gain as well as a good VSWR profile over the entire operating band for WiMAX and 5G communications.

4. Conclusion

A compact single band antenna with a wide operating frequency range (3.10–4.50 GHz) for WiMAX (3.4–3.6 GHz) and lower 5G (3.3–4.2 GHz) communications has been designed and analyzed in this paper. The proposed compact design provides improved antenna radiation parameters such as peak gain and directivity of 3.90 dB and 4.20 dBi, respectively. It also produces a preferable reflection coefficient of -46.78 dB at the center operating frequency of 3.592 GHz and has an excellent impedance matching property. The low profile compact antenna maintains a high efficiency range of 94–98% over the wide operating band with a good VSWR profile. The presented simulated and experimental results show the usefulness of the designed compact antenna for the intended applications.

Data Availability

The data used to support the findings of this study are included within the article.

Conflicts of Interest

The authors declare no potential conflict of interests.

References

[1] A. Kaur and P. K. Malik, "Adoption of micro-strip patch antenna for wireless communication," *Engineering*, vol. 10, no. 1, pp. 1–21, 2021.

[2] K. Shafique, B. A. Khawaja, F. Sabir, S. Qazi, and M. Mustaqim, "Internet of Things (IoT) for next-generation smart systems: a review of current challenges, future trends and prospects for emerging 5G-IoT scenarios," *IEEE Access*, vol. 8, pp. 23022–23040, 2020.

[3] A. Narayanan, A. S. D. Sena, D. Gutierrez-Rojas et al., "Key advances in pervasive edge computing for Industrial Internet of Things in 5G and beyond," *IEEE Access*, vol. 8, pp. 206734–206754, 2020.

[4] A. A. Salih, S. R. Zeebaree, A. S. Abdulraheem, R. R. Zebari, M. A. Sadeeq, and O. M. Ahmed, "Evolution of mobile wireless communication to 5G revolution," *Technology Reports of Kansai University*, vol. 62, no. 5, pp. 2139–2151, 2020.

[5] I. A. Gedel and N. I. Nwulu, "Low latency 5G distributed wireless network architecture: a techno-economic comparison," *Inventions*, vol. 6, no. 1, p. 11, 2021.

[6] E. Iradier, A. Abuin, L. Fanari, J. Montalban, and P. Angueira, "Throughput, capacity and latency analysis of P-NOMA RRM schemes in 5G URLLC," *Multimedia Tools and Applications*, vol. 81, no. 9, pp. 12251–12273, 2022.

[7] E. K. Kumari, M. V. Kumar, P. K. Sharma, and S. Murugan, "Double-sided split ring resonator-based probe feed patch antenna with enhanced bandwidth for 5G and Ku band applications," *Communication and Intelligent Systems: Proceedings of ICCIS*, vol. 204, pp. 461–474, 2021.

[8] W.-H. Chang, S.-W. Su, and B.-C. Tseng, "Self-decoupled, 5G NR77/78/79 two-antenna system for notebook computers," in *2019 Electrical Design of Advanced Packaging and Systems (EDAPS)*, pp. 1–3, Kaohsiung, Taiwan, December 2019.

[9] S. Khorashadizadeh, A. R. Ikuesan, and V. R. Kebande, "Generic 5G infrastructure for IoT ecosystem," in *Emerging Trends in Intelligent Computing and Informatics: Data Science, Intelligent Information Systems and Smart Computing 4: Proceedings of IRICT 2019*, vol. 1073, pp. 451–462, Johor, Malaysia, 2019.

[10] A. Musa and B. S. Paul, "Simulation of WiMAX and logical segmentation of its application," in *2019 IEEE Africon*, pp. 1–5, Accra, Ghana, September 2019.

[11] A. A. Akinlabi and F. M. Dahunsi, "Mobile broadband quality of service analysis using host-based performance measurements," *African Journal of Science, Technology, Innovation and Development*, vol. 14, no. 4, pp. 1083–1101, 2022.

[12] M. Tabassum, M. K. Haldar, and D. F. S. Khan, "Implementation and performance evaluation of advance metering infrastructure for Borneo-wide power grid," *Frontiers in Energy*, vol. 14, no. 1, pp. 192–211, 2020.

[13] M. Pandimadevi and R. Tamilselvi, "Design and fabrication of flexible antenna using foam substrate for WiMAX applications," in *Micro-Electronics and Telecommunication Engineering: Proceedings of 4th ICMETE 2020*, pp. 191–202, Johor, Malaysia, 2021.

[14] K. Abdalgader and D. K. Saini, "Data streams scheduling approach for WiMAX networks," *The Journal of Communication*, vol. 15, no. 6, pp. 469–479, 2020.

[15] R. Astya and P. K. Mishra, "Review on evolution of mobile WiMAX model," *Journal of Critical Reviews*, vol. 7, no. 3, pp. 785–789, 2020.

[16] H. Prasad and M. J. Akhtar, "Flexible substrate based CPW-fed antenna for WiMAX application," in *2017 IEEE Applied Electromagnetics Conference (AEMC)*, pp. 1-2, Aurangabad, India, December 2017.

[17] H. Zerrouki and S. Azzaz-Rahmani, "WiMAX throughput maximization for MIMO-OFDM systems via cross-layer design," in *WITS 2020: Proceedings of the 6th Int'l Conf. on Wireless Technologies, Embedded, and Intelligent Systems*, pp. 921–931, Johor, Malaysia, 2022.

[18] A. E. Hamraoui, E. H. Abdelmounim, J. Zbitou, L. Elabdellaoui, H. Bennis, and M. Latrach, "A new compact CPW-fed dual-band uniplanar antenna for RFID applications," *TELKOMNIKA (Telecommunication Computing Electronics and Control)*, vol. 16, no. 1, pp. 102–109, 2018.

[19] G. Jin, C. Deng, J. Yang, Y. Xu, and S. Liao, "A new differentially-fed frequency reconfigurable antenna for WLAN and sub-6GHz 5G applications," *IEEE Access*, vol. 7, pp. 56539–56546, 2019.

[20] A. R. Cheekatla and D. P. S. Ashtankar, "Compact micro strip antenna for 5G mobile phone applications," *International Journal of Applied Engineering Research*, vol. 14, no. 2, pp. 108–111, 2019.

[21] M. Yerlikaya, S. S. Gültekin, and D. Uzer, "A novel design of a compact wideband patch antenna for sub-6 GHz fifth-generation mobile systems," *International Advanced Researches and Engineering Journal*, vol. 4, no. 2, pp. 129–133, 2020.

[22] Y. Al-Yasir, A. Abdullah, N. O. Parchin, R. Abd-Alhameed, and J. Noras, "A new polarization-reconfigurable antenna for 5G applications," *Electronics*, vol. 7, no. 11, p. 293, 2018.

[23] S. Nelaturi, "ENGTL based antenna for Wi-Fi and 5G," *Analog Integrated Circuits and Signal Processing*, vol. 107, no. 1, pp. 165–170, 2021.

[24] J. Iqbal, U. Illahi, M. N. M. Yasin, M. A. Albreem, and M. F. Akbar, "Bandwidth enhancement by using parasitic patch on dielectric resonator antenna for sub-6 GHz 5G NR bands application," *Alexandria Engineering Journal*, vol. 61, no. 6, pp. 5021–5032, 2022.

[25] A. Kapoor, R. Mishra, and P. Kumar, "Compact wideband-printed antenna for sub-6 GHz fifth-generation applications," *International Journal on Smart Sensing and Intelligent Systems*, vol. 13, no. 1, pp. 1–10, 2020.

[26] H. Singh, N. Mittal, A. Gupta, Y. Kumar, M. Woźniak, and A. Waheed, "Metamaterial integrated folded dipole antenna with low SAR for 4G, 5G and NB-IoT applications," *Electronics*, vol. 10, no. 21, p. 2612, 2021.

[27] M. Khalifa, L. Khashan, H. Badawy, and F. Ibrahim, "Broadband printed-dipole antenna for 4G/5G smartphones," *Journal of Physics: Conference Series*, vol. 1447, no. 1, article 012049, 2020.

[28] R. Swetha and A. Lokam, "Novel design and characterization of wide band hook shaped aperture coupled circularly polarized antenna for 5G application," *Progress In Electromagnetics Research C*, vol. 113, pp. 161–175, 2021.